Electron Transport Phenomena in Bismuth at Liquid-Helium Temperatures*†

C. G. GRENIER, J. M. REYNOLDS, AND J. R. SYBERT
Louisiana State University, Baton Rouge, Louisiana
(Received 25 April 1963)

Transport effects were studied in a bismuth single crystal at liquid-helium temperatures in a magnetic field. Except for a field-orientation study of the galvanomagnetic effects for mapping the light-holes ellipsoid, all the measurements were taken in the basal plane of the crystal with the field parallel to the trigonal axis. The thermal conductivity was found to be almost entirely due to lattice conductivity; therefore, the experimental coefficients determined were limited to the following: the isothermal transverse magnetoresistivity ρ_{11}, the isothermal Hall resistivity ρ_{21}, the (adiabatic) thermoelectric coefficient ϵ_{11}', the (adiabatic) Nernst-Ettinghausen coefficient ϵ_{21}', and the transverse magnetothermal resistivity γ_{11}. The Peltier tensor coefficients were expected (from the Onsager relations) to be too small to be measurable and thus, were not studied here. All these effects, except the thermal resistivity coefficient exhibit the Schubnikov-de Haas type oscillations. The kinetic coefficients of the transport effects σ_{11}, σ_{12}, ϵ_{11}'', and ϵ_{12}'' were computed from the experimental coefficients and compared with available theories. A rough analysis of the gross effects was made by a decomposition of each coefficient into a sum of different band contributions, each band being approximated by a Lorentz term. General, but not complete, agreement between experiment and theory is achieved for both two-band and multiband models. No special mechanism (i.e., like that proposed for zinc) is needed to explain the oscillations in the different effects, since the Lifshitz and Kosevich theory (σ_{12}), the Zil'berman theory (σ_{11},ϵ_{11}''), and the influence of oscillation in the density of states (ϵ_{12}'') lead to satisfactory agreement with the experiments.

I. INTRODUCTION

TO obtain information on the band structure of bismuth, galvanomagnetic and thermomagnetic potentials were measured in a single crystal at liquid-helium temperatures. The de Haas–van Alphen (dHvA) type oscillations observed were readily analyzed, yielding information on the various bands of carriers. The gross effects upon which the oscillations are superimposed were analyzed for information on the different carriers, particularly for the possible existence of heavy carriers which show no oscillations in the temperature range studied.

In recent years, extensive investigations have been made to determine the electronic nature of bismuth. These studies include galvanomagnetic effects,[1–7] anomalous skin effect,[8] ultrasonic attenuation,[9] cyclotron resonance,[10–13] de Haas–van Alphen[14–17] and Shubnikov–de Haas effects,[18–23] specific heat,[24,25] and others.[26–28]

The available data lead to a model of the Fermi surface (FS), but there remain several discrepancies. Many of the parameters associated with the different bands of carriers are known only in order of magnitude, or within a multiplicative factor. The present work examines the galvano- and thermomagnetic effects both individually and collectively in order to add to the present model of the FS.

A model for the electronic part of the FS was first established from de Haas–van Alphen oscillations.[14] This portion of the FS consists of three ellipsoids (in momentum space) lying almost in the basal plane [the (1)–(2) plane of Fig. 1] and interrelated by 120° rotations about the principal axis. Inversion symmetry in the first-Brillouin zone allows for doubling these electron ellipsoids; this doubling is probable, although

* This work was supported by the U. S. Army Research Office, Durham.

† Part of this work was submitted (by J.R.S.) in partial fulfillment of the requirements for the Ph.D. degree at Louisiana State University.

[1] B. Abeles and S. Meiboom, Phys. Rev. **101**, 544 (1956).
[2] A. L. Jain, Phys. Rev. **114**, 1518 (1959).
[3] T. Okada, Mem. Fac. Sci. Kyusyu Univ. **B1**, 168 (1955).
[4] A. L. Jain and S. H. Koenig, Phys. Rev. **127**, 442 (1962).
[5] S. Mase and S. Tanuma, J. Phys. Soc. Japan **14**, 1644 (1959).
[6] Schoichi Mase, S. Von Molnar, and A. W. Lawson, Phys. Rev. **127**, 1030 (1962).
[7] R. N. Zitter, Phys. Rev. **127**, 1471 (1962).
[8] George E. Smith, Phys. Rev. **115**, 1561 (1959).
[9] D. H. Reneker, Phys. Rev. **115**, 303 (1959).
[10] I. E. Aubrey and R. G. Chambers, J. Phys. Chem. Solids **3** 128 (1957).
[11] I. E. Aubrey, J. Phys. Chem. Solids **19**, 321 (1961).
[12] J. K. Galt, W. A. Yager, F. R. Merritt, B. B. Celtin, and A. D. Brailsford, Phys. Rev. **114**, 1396 (1959).
[13] Glen E. Everett, Phys. Rev. **128**, 2564 (1962).
[14] D. Shoenberg, Phil. Trans. **A245**, 1 (1952).
[15] N. V. Brandt, A. E. Dubrovskaya, and G. A. Kytin, Zh. Eksperim. i Teor. Fiz. **37**, 572 (1959) [translation: Soviet Phys.—JETP **10**, 405 (1960)].
[16] N. V. Brandt, Zh. Eksperim. i Teor. Fiz. **38**, 1355 (1960) [translation: Soviet Phys.—JETP **11**, 975 (1960)].
[17] D. Weiner, Phys. Rev. **125**, 1226 (1962).
[18] J. M. Reynolds, H. W. Hemstreet, T. E. Leinhardt, and D. D. Triantos, Phys. Rev. **96**, 1203 (1954).
[19] P. B. Alers and R. T. Webber, Phys. Rev. **91**, 1060 (1953).
[20] J. Babiskin, Phys. Rev. **107**, 981 (1957).
[21] R. A. Connell and J. A. Marcus, Phys. Rev. **107**, 940 (1957).
[22] W. C. Overton and T. G. Berlincourt, Phys. Rev. **99**, 1165 (1955).
[23] L. S. Lerner, Phys. Rev. **127**, 1480 (1962).
[24] I. N. Kalinkina and P. G. Strelkov, Zh. Eksperim. i Teor. Fiz. **34**, 616 (1958) [translation: Soviet Phys.—JETP **7**, 426 (1958)].
[25] N. E. Phillips, Phys. Rev. **118**, 644 (1960).
[26] M. C. Steele and J. Babiskin, Phys. Rev. **98**, 359 (1955).
[27] J. R. Sybert, C. G. Grenier, and J. M. Reynolds, Bull. Am. Phys. Soc. **7**, 74 (1962).
[28] C. Gallo, B. S. Chandrasekhar, and P. H. Sutter, J. Appl. Phys. (to be published).

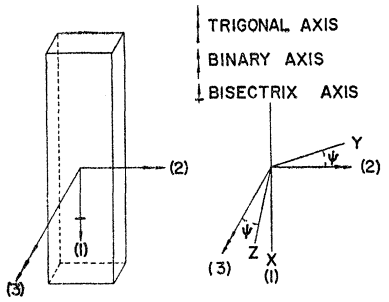

FIG. 1. The symmetry axes in the bismuth crystal. ψ is the angle between the magnetic field H and the trigonal axis (3) in the (3)–(2) plane.

not firmly established experimentally. These electrons are apparently the most mobile carriers in bismuth.

A FS of relatively high-mobility holes has the form of an ellipsoid of revolution centered on the principal (trigonal) axis with its major axis in the trigonal direction.[1,15] A multiplicity of two for this pocket of carriers is also possible, but rather improbable as there is recent evidence for a single pocket.[17,4,28,29]

In addition to the relatively high-mobility holes and electrons, there is evidence of other carriers—probably holes—of quite low mobility.[23,27] These heavy carriers have an approximately spheroidal FS,[23] and a density-of-states effective mass, m^*, of the order of the free-electron mass m_0. A fourth band of carriers with even lower mobility may also exist.[23,27]

II. NOTATION AND CONVENTIONS

The transport effects are described in kinetic theory by the relations

$$\begin{aligned}\mathbf{J}&=\hat{\sigma}\mathbf{E}^*-\hat{\epsilon}''\mathbf{G},\\ \mathbf{w}^*&=-\hat{\pi}''\mathbf{E}^*+\hat{\lambda}''\mathbf{G},\end{aligned}\tag{1}$$

where $\mathbf{J}$ is the electric-current density and $\mathbf{G}$ is the negative-temperature gradient. The quantities $\mathbf{E}^*$ and $\mathbf{w}^*$ are the electric-field and heat-current density, respectively, each modified for convenience by a term involving the chemical potential μ_c. The expressions are[30,31]

$$\begin{aligned}\mathbf{E}^*&=\mathbf{E}+e^{-1}\,\mathrm{grad}\mu_c,\\ \mathbf{w}^*&=\mathbf{w}+e^{-1}\mu_c\mathbf{J},\end{aligned}$$

where $\mathbf{E}$ is the electrostatic field, $\mathbf{w}$ is the heat-current density, and e is the magnitude of the electronic charge (a positive number). The quantities $\hat{\sigma}$, $\hat{\epsilon}''$, $\hat{\pi}''$, and $\hat{\lambda}''$ are tensors relating the "fluxes" $\mathbf{J}$ and $\mathbf{w}^*$ with the "affinities" $\mathbf{E}^*$ and $\mathbf{G}$.

Other relations between $\mathbf{J}$, $\mathbf{w}^*$, $\mathbf{E}^*$, and $\mathbf{G}$

$$\begin{aligned}\mathbf{E}^*&=\hat{\rho}\mathbf{J}+\hat{\epsilon}\mathbf{G},\\ \mathbf{w}^*&=-\hat{\pi}\mathbf{J}+\hat{\lambda}\mathbf{G},\end{aligned}\tag{2}$$

and

$$\begin{aligned}\mathbf{E}^*&=\hat{\rho}'\mathbf{J}+\hat{\epsilon}'\mathbf{w}^*,\\ \mathbf{G}&=\hat{\pi}'\mathbf{J}+\hat{\gamma}\mathbf{w}^*,\end{aligned}\tag{3}$$

are often used. This threefold representation allows computation of the tensor elements in the more convenient form of Eq. (1) from the experimentally determined quantities $\hat{\rho}$, $\hat{\epsilon}'$, $\hat{\pi}'$, and $\hat{\gamma}$. The expressions for the tensors in Eq. (1) in terms of the experimental quantities are

$$\begin{aligned}\hat{\sigma}&=\hat{\rho}^{-1},\\ \hat{\lambda}&=\hat{\gamma}^{-1},\\ \hat{\epsilon}''&=\hat{\sigma}\hat{\lambda}\hat{\epsilon}',\\ \hat{\lambda}''&=\hat{\lambda}+\hat{\epsilon}\hat{\pi}'',\\ \hat{\pi}''&=\hat{\sigma}\hat{\lambda}\hat{\pi}'.\end{aligned}\tag{4}$$

The elements of $\hat{\sigma}$, $\hat{\epsilon}''$, and $\hat{\lambda}$ reported in this investigation were calculated by means of Eq. (4). The nomenclature for the transport coefficients is as follows: The condition $G_2=0$ is called "isothermal"; that of $w_2^*=0$ is called "adiabatic." Thus we refer to ϵ_{11}, ϵ_{11}', and ϵ_{11}'' as the isothermal thermoelectric coefficient, the adiabatic-thermoelectric coefficient and the kinetic-thermoelectric coefficient, respectively. Similarly, ϵ_{12} is the isothermal Ettinghausen-Nernst (E-N) coefficient; ϵ_{12}', the adiabatic E-N coefficient; and ϵ_{12}'', the kinetic E-N coefficient.

The experimental transport coefficients $\hat{\rho}$, $\hat{\epsilon}$, and $\hat{\gamma}$ were obtained with the magnetic field applied parallel to the principal axis of the crystal. With this geometry and the symmetry of the bismuth crystal, these tensors have the form

$$a=\begin{bmatrix} a_{11} & a_{12} & 0\\ -a_{12} & a_{11} & 0\\ 0 & 0 & a_{33}\end{bmatrix},$$

and have the following symmetries with respect to the magnetic field H:

$$\begin{aligned}a_{12}(H)&=-a_{12}(-H),\\ a_{11}(H)&=a_{11}(-H).\end{aligned}$$

The two elements a_{11} and a_{12} are the ones of interest in the present investigation since measurements were made in the basal plane. Since these coefficients generally exhibit Schubnikov–de Haas type oscillations, the notation $\bar{a}_{\alpha\beta}$, $\tilde{a}_{\alpha\beta}$ is used to distinguish between the gross effect and the oscillatory part of the effects. The amplitude of the oscillations is denoted by $|\tilde{a}_{\alpha\beta}|$.

III. EXPERIMENT

A. The Crystal

The crystal was prepared from spectroscopically pure bismuth obtained from Johnson, Mathey, and Company. It was first grown as an ingot without preorientation and then cut to shape. The finished

[29] G. E. Smith, J. Phys. Chem. Solids **20**, 168 (1961).
[30] H. B. Callen, *Thermodynamics* (John Wiley & Sons, Inc., New York, 1960).
[31] J. P. Jan, in *Solid State Physics*, edited by F. Sitz and D. Turnbull (Academic Press Inc., New York, 1957), Vol. 5, p. 1.

specimen had the form of a right parallelepiped with dimensions 24.3 mm×6.9 mm×2.5 mm. The crystal had a resistance ratio $R(300°K)/R(4.2°K)\simeq 40$. This low purity was found to be advantageous as will be seen in the analysis of the results. The orientation of the symmetry axes in the specimen is shown in Fig. 1. With the exception of the galvanomagnetic orientation studies performed with the magnetic field in the (2)–(3) plane, all measurements of galvano- and thermomagnetic potentials were made in the (1)–(2) plane with the magnetic field directed along the 3 axis.

B. Measuring Techniques

A chamber was constructed to provide a crystal suspension system by which both galvano- and thermomagnetic potentials could be measured without disturbing the contact with the crystal. Carbon-resistance thermometers encased in thin copper sleeves were attached by stiff copper leads directly to the crystal. A solder composed of bismuth, tin, and lead was used to make connections to the crystal. Electric potential leads of No. 40 gauge wire were then soldered to the stiff thermal leads to give common contact points for both types of measurements. The leads were brought out of the vacuum chamber into the liquid helium through a seal of epoxy resin.[32] Thermomagnetic measurements were made in a vacuum better than 5×10^{-6} mm Hg. The isothermal condition for the galvanomagnetic measurements was achieved by allowing the surrounding liquid helium to fill the vacuum chamber. Potentials were measured by a dc method described by Bergeron, Grenier, and Reynolds.[33]

C. Experimental Data

The Hall resistivity ρ_{21} and magnetoresistivity ρ_{11} are shown in Fig. 2 for magnetic fields up to 17 kG and temperatures 2.1 and 4.2°K. The curves exhibit the characteristic Schubnikov–de Haas oscillations in $1/H$. With the field in the (3) direction, the only detectable oscillations are those due to the light hole pocket. The thermoelectric coefficients $\epsilon_{\alpha\beta}'$ are shown in Fig. 3; the temperature dependence is to be noted. Both ρ_{21} and ϵ_{11} show a change in sign near 1500 G. In the case of ρ_{21}, the change of sign means that $(\pm)n_j>0$, i.e., the number of holes slightly exceeds the number of electrons. In the case of ϵ_{11}', it indicates a low-mobility hole carrier with a large density of states. Neither $\rho_{\alpha\beta}$ nor $\epsilon_{\alpha\beta}'$ are analyzed directly, but rather are used together with data on the thermal conductivity from Fig. 8 to construct $\epsilon_{\alpha\beta}''$ and $\sigma_{\alpha\beta}$.

It is important to note that the experimental data obtained for $\epsilon_{\alpha\beta}'$ are related to the bismuth-copper thermocouple formed by the bismuth crystal and the copper leads. The effect of the absolute "isothermal" thermoelectric power of the copper leads ϵ_{Cu} is to modify the expression for $\hat{\epsilon}$.[34] The experimentally determined ϵ' is given by

$$\hat{\epsilon}'=\hat{\lambda}^{-1}(\hat{\epsilon}-\mathbf{1}\epsilon_{Cu}).$$

The value $\epsilon_{Cu}\simeq 0.8\times10^{-6}$ V/deg reported by Blatt and Kropschot[35] when compared to our value $\lambda_{11}\epsilon_{11}'=34.6\times10^{-6}$ V/deg (both with $H=0$ at 4.2°K) indicates that the effect of the copper would be less than 2% of the total; the value $\epsilon_{Cu}=-3.2\times10^{-8}$ V/deg at $H=0$ and $T=4.2$°K for similar copper leads as reported by Grenier, Reynolds, and Zebouni,[34] yields an effect still smaller. In the later analysis, the effect of the thermoelectric power of the copper leads is neglected.

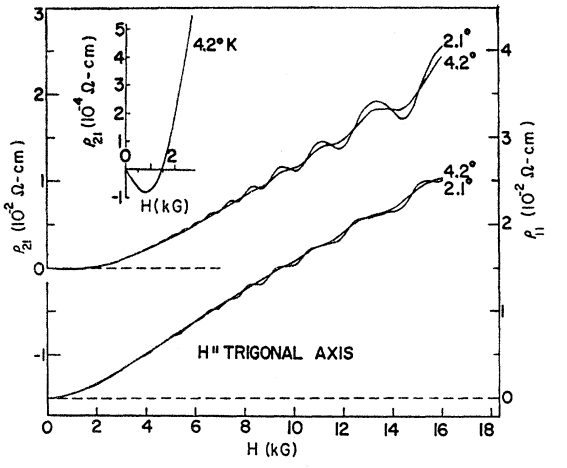

FIG. 2. Hall resistivity and magnetoresistivity of the sample at 4.2 and 2.1°K for $\psi=0$. The upper two curves are for ρ_{21}, the lower two for ρ_{11}. The insert shows the sign inversion occurring in ρ_{21} at low field.

IV. THEORY

A. Modified Sondheimer-Wilson Theory

The monotonic parts of both $\sigma_{\alpha\beta}$ and $\epsilon_{\alpha\beta}''$ are analyzed in terms of a modified Sondheimer-Wilson theory.[36] The expressions obtained assume a quasicontinuum of states in "parabolic" bands with sharp Fermi distribution functions and isotropic relaxation time independent of energy. Under these conditions, the conductivities are given by

$$\begin{aligned}\sigma_{12}/H&=(ec)\sum(\pm)n_jL_j,\\ \sigma_{11}&=(ec)\sum a_jn_jH_jL_j,\end{aligned}\qquad(5)$$

where the summation extends over all bands and the (+) sign is taken for holes and (−) for electrons. Here, $H_j=cm_j^*/e\tau_j$ is a quantity inversely proportional to

[32] K. S. Balain, C. J. Bergeron, Rev. Sci. Instr. **30**, 1058 (1959).
[33] C. J. Bergeron, C. G. Grenier, and J. M. Reynolds, Phys. Rev. **119**, 925 (1960).
[34] C. G. Grenier, J. M. Reynolds, and N. H. Zebouni, Phys. Rev. **129**, 1088 (1963).
[35] F. J. Blatt and R. N. Kropschot, Phys. Rev. **118**, 480 (1960).
[36] A. H. Wilson, *The Theory of Metals* (Cambridge University Press, New York, 1954).

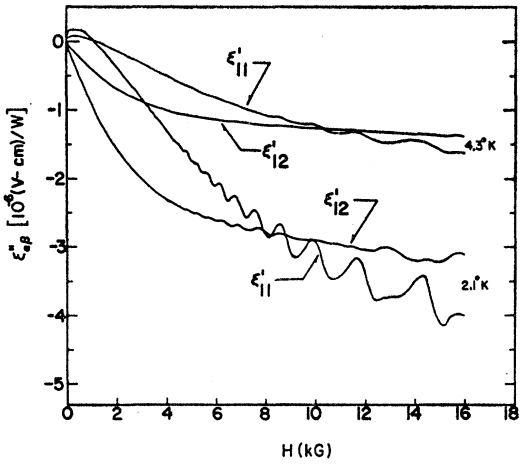

FIG. 3. The adiabatic-thermoelectric coefficients ϵ_{11}' and ϵ_{12}'. Experimental values were obtained with H parallel to trigonal axis ($\psi=0$) at 4.3 and 2.1°K.

the mobility at zero field and is hereafter called the saturation field; L_j is the Lorentz term $L_j=(H^2+H_j^2)^{-1}$; n_j is the number of carriers; τ_j is the relaxation time; and the subscript j indicates that these definitions apply to the jth band. The factor a_j is an adjustable parameter introduced to correct for noncircular orbits[37]; for circular orbits, a_j is equal to one.

Under the above conditions and with the additional assumption that the relaxation times for electrical and thermal processes are equal, a second-order approximation for the Fermi function at finite temperature gives for $\epsilon_{\alpha\beta}''$,

$$\begin{aligned}\epsilon_{12}''/H&=-(\tfrac{1}{3}\pi^2k^2cT)\sum b_jZ_j^0L_j,\\ \epsilon_{11}''&=-(\tfrac{1}{3}\pi^2k^2cT)\sum(\pm)c_jZ_j^0H_jL_j,\end{aligned}\tag{6}$$

where Z_j^0 is the density of states in band j at zero field. Here b_j and c_j are adjustable parameters introduced to facilitate curve fitting. Ideally, b_j should equal one and c_j should equal a_j.

Since real metals do not necessarily satisfy the conditions under which Eqs. (5) and (6) are derived, those equations may need to be modified empirically to fit the data. Possible modifications are: (1) The decomposition of a band into several subbands; (2) the spreading of a band into a continuum, and (3) the shifting of a band by considering the saturation field H_j to be field-dependent. In the analysis of these data, no such modification was considered; a match of each band by a single Lorentz term of the type of Eqs. (5) and (6) was attempted.

B. Lifshitz-Kosevich Theory of Oscillations in the Galvanomagnetic Effects

A large amount of information comes from a detailed study of the dHvA type oscillations which occur at high-magnetic fields. For an understanding of the transport processes, one must explain the scattering mechanism and their magnetic-field dependence. As yet, a theory has not been devised which approaches the excellence of the theory of the de Haas–van Alphen effect. Attempts have been made, however, to obtain a theory of the Shubnikov–de Haas oscillation, first by Levinger and Grimsal[38] and more recently by Lifshitz and Kosevich,[39] who related the field-dependent oscillations in the conductivity tensor $\sigma_{\alpha\beta}$ to the susceptibility oscillations through the classical mobility tensor. Zil'berman[40] and others[41–42] have also studied the influence of Landau quantization on various galvanomagnetic and thermomagnetic effects. The Zil'berman theory is discussed in Sec. IVD.

In the Lifshitz-Kosevich theory, the oscillatory part of the conductivity tensor is written as

$$(\tilde{\sigma}_{\alpha\beta})_{\text{L–K}}=\Delta\sigma_{\alpha\beta}+\Delta_1\sigma_{\alpha\beta},\tag{7}$$

where the first term arises from magnetic field-dependent oscillations in the number of carriers in the various bands under the assumption of a constant Fermi energy ζ. The second term comes from oscillations in the number of carriers in the different bands with varying ζ but with $\sum_j(\pm)n_j$ assumed constant. With $q_{m_j}{}^{\alpha\beta}$ denoting the classical mobility tensor for the carriers at the extremal cross-sectional area of the jth pocket (band) perpendicular to the applied field, the first term in Eq. (17) is written as

$$\Delta\sigma_{\alpha\beta}=\sum q_{m_j}{}^{\alpha\beta}\tilde{n}_j,\tag{8}$$

where $\tilde{n}_j$ is the oscillation in the number of carriers in the jth band. The explicit expression for $\tilde{n}$ for a pocket of carriers with an ellipsoidal FS with major axis parallel to H is [38,39,43,44]

$$\tilde{n}=4pRh^{-3}\left(\frac{e\hbar H}{c}\right)^{3/2}\sum_\kappa\kappa^{-2/3}\left(\frac{\kappa\lambda}{\sinh\kappa\lambda}\right)\times\exp\left[i\kappa\left(\frac{c}{e\hbar H}\right)S_m-i(2\pi\kappa\gamma+\tfrac{3}{4}\pi)\right],\tag{9}$$

[37] In case of a set of tilted ellipsoids defined by the mass tensor

$$\hat{m}=\begin{bmatrix}m_1&0&0\\0&m_2&m_4\\0&m_4&m_3\end{bmatrix},$$

a is equal to $\frac{1}{2}(m_1+m_2-m_4^2m_3^{-1})(m_2m_3-m_4^2)^{-1/2}\times m_1^{-1/2}m_3^{+1/2}$. If the set is defined through the inverse mass tensor

$$\begin{bmatrix}\alpha_1&0&0\\0&\alpha_2&\alpha_4\\0&\alpha_4&\alpha_3\end{bmatrix},$$

then a is simply $\frac{1}{2}(\alpha_1/\alpha_2)^{1/2}+(\alpha_2/\alpha_1)^{1/2}$; and if the ratio R_e between the principal axes of the basal cross section of the ellipsoid is known, then a is simply $\frac{1}{2}(R_e+R_e^{-1})$.

[38] J. S. Levinger and E. G. Grimsal, Phys. Rev. **94**, 772 (1954).
[39] I. Lifshitz and L. M. Kosevich, Zh. Eksperim. i Teor. Fiz. **33**, 88 (1957) [translation: Soviet Phys.—JETP **6**, 67 (1958)].
[40] G. E. Zil'berman, Zh. Eksperim. i Teor. Fiz. **29**, 762 (1955) [translation: Soviet Phys.—JETP **2**, 650 (1959)].
[41] List of references can be found in the review article by A. H. Kahn and H. P. R. Frederikse, in *Solid State Physics*, edited by F. Seitz and P. Turnbull (Academic Press Inc., New York, 1960), Vol. 9.
[42] P. Horton (private communication).
[43] I. M. Lifshitz and L. M. Kosevich, Zh. Eksperim. i Teor. Fiz. **29**, 730 (1955) [translation: Soviet Phys.—JETP **2**, 636 (1956)].
[44] R. B. Dingle, Proc. Roy. Soc. (London) **A211**, 500 (1952).

where p is the multiplicity of the ellipsoids, R is the ratio of major to minor axis of the ellipsoid(s), S_m is the extremal cross-sectional area (of the ellipsoid) perpendicular to the magnetic field, λ is $2\pi^2 km^* cT/e\hbar H$, γ is a parameter defined such that $\gamma c/ehH$ is the area of the lowest Landau level and is equal to one-half for free electrons, and k is Boltzmann's constant. Note that the period in $1/H$ is

$$P=\Delta(1/H)=eh/cS_m. \tag{10}$$

The second term in Eq. (7) is

$$\Delta_1\sigma_{\alpha\beta}=-\left[\sum_i\left(\frac{\partial\langle q_i^{\alpha\beta}\rangle_{\rm av}}{\partial\zeta_0}\right)N_i^0+\sum_i\langle q_i^{\alpha\beta}\rangle_{\rm av}Z_i^0\right]\times\left[\sum_i Z_i^0\right]^{-1}\sum_j\tilde{n}_j, \tag{11}$$

where i and j are summed over all bands, $\langle q_i^{\alpha\beta}\rangle_{\rm av}$ is the average classical-mobility-tensor coefficient of the ith band carriers. Here, N_i^0 denotes the number of states in band i, where the zero refers to zero magnetic field.

C. Oscillation in the Density of States and in the Thermoelectric Effects

In the absence of a theory for Landau quantization in the Nernst-Ettingshausen effect, the classical expression Eq. (6) is applied directly. Thus, the oscillations in the density of states $\tilde{Z}$ is expected to give a contribution to the oscillatory part of the thermoelectric tensor $\tilde{\epsilon}_{\alpha\beta}''$ of the form

$$(\tilde{\epsilon}_{\alpha\beta}'')_{\rm d.s.}=\sum\epsilon_{\alpha\beta j}''\tilde{Z}_j/Z_j^0, \tag{12}$$

where $\epsilon_{\alpha\beta j}''$ is the jth term in Eq. (6) and $\tilde{Z}=\partial\tilde{n}/\partial\zeta$.

D. Zil'berman Theory for Oscillations in the Conductivity Coefficient $\tilde{\sigma}_{11}$ and the Thermoelectric Coefficient $\tilde{\epsilon}_{11}''$

The influence of Landau quantization on electron scattering on lattice imperfections has been studied by Zil'berman in the effective mass approximation with complete isotropy. The amplitude of oscillations in the conductivity coefficient $|\tilde{\sigma}_{11}|$ and in the thermoelectric coefficient $|\tilde{\epsilon}_{11}''|$ can be written for band j in a first-harmonic approximation

$$|\tilde{\sigma}_{11}|_{\rm Zil}=\sigma_{11j}\left(\frac{5}{4}\sqrt{2}\right)\left(\frac{\lambda_j}{\sinh\lambda_j}\right)(P_jH)^{1/2}, \tag{13}$$

$$|\tilde{\epsilon}_{11}''|_{\rm Zil}=\epsilon_{11j}''(5\pi\sqrt{2})\left(\frac{1-\lambda_j\coth\lambda_j}{\lambda_j\sinh\lambda_j}\right)(P_jH)^{-1/2}, \tag{14}$$

where σ_{11j} and ϵ_{11j}'' are given as the jth terms of Eqs. (5) and (6), respectively. The above equations are the results of a modification of the Zil'berman theory by Horton.[42]

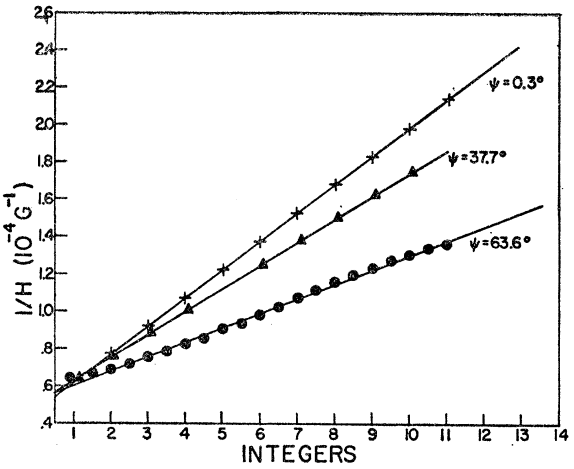

FIG. 4. Typical plots of $1/H$ at successive maxima (or minima) of the Shubnikov–de Haas oscillations versus integers (or half-integers) for different orientations of the magnetic field in the (3)–(2) plane.

It may be noted that when the oscillations are small, the expressions Eqs. (13) and (14) simply add to the contributions from Eqs. (7) and (12) since the sources of the oscillations are different in the two cases.

V. RESULTS

A. The Light-Hole Ellipsoid

The high-mobility hole pocket was mapped in detail first by Brandt from dHvA oscillations[16] and then by the present authors from galvanomagnetic oscillations in the early stages[45] of this study. Other experimental techniques previously had established some of the parameters of this pocket.[1,8,12,18] In this investigation, oscillations in the resistivity tensor elements $\rho^{\alpha\beta}$ for various magnetic-field orientations in the (2)–(3) plane were observed at 1.8°K in fields ranging up to 16 kG. The dimensions of the ellipsoid are established by computing S_m for various orientations ψ from Eq. (10). Here ψ is the angle [in the (2)–(3) plane] between the (3) axis and the applied magnetic field as shown in Fig. 1. The periods were determined by examination of the recorder traces for maxima and minima. The values of $1/H$ corresponding to successive maxima were plotted against successive integers; the slope of the resulting curve determined the value of the period. Typical plots are shown in Fig. 4. The oscillations observed are due not only to the hole ellipsoid under investigation, but also to other pockets of carriers. The presence of one of the high-mobility electron ellipsoids mapped by Shoenberg can be seen in the $\psi=63.6°$ plot where it shows up as a periodic error in the determination of the shorter period due to the holes (see next section). Since an extensive mapping of the electrons pockets has

[45] J. R. Sybert, C. G. Grenier, and J. M. Reynolds, Bull. Am. Phys. 6, 461 (1961).

already been made, no attempt is made here to analyze the oscillations due to the electrons. Only a few periods were checked and found in perfect agreement with the Shoenberg[14] or Lerner[23] data. For a prolate ellipsoid of revolution, Eq. (10) can be written in the form

$$P^2=(eh/\pi ac)^2[(a^{-2}-c^{-2})\cos^2\psi+c^{-2}], \qquad (15)$$

where a and c are the semiminor and semimajor axes, respectively. A plot of P^2 as a function of $\cos^2\psi$ is shown in Fig. 5. The linearity of the curve indicates that the FS of the light holes is indeed ellipsoidal. There is evidence from the work of Brandt *et al.*[15] of a departure of the FS from an ellipsoid for values of $\psi>75°$ (just beyond the range of our measurements). However, this departure was not mentioned in a later publication concerning, presumably, the same experimental data.[16] The period for $\psi=0$ is 1.52×10^{-5} G^{-1} and the period extrapolates to 0.43×10^{-5} G^{-1} for $\psi=90°$. The volume of the ellipsoid in momentum space is found to be $V=4.97\times10^{-62}$ (g cm/sec)^3; the number of holes per atom per ellipsoid is 1.21×10^{-5} per atom or 3.43×10^{17} per cm^3 in good agreement with data of Brandt *et al.*

The temperature dependence of the oscillations in the $\sigma^{\alpha\beta}$ (with $\psi=0$) is the same as that in n as given by Eq. (9). For constant H, the values of the effective mass m^* and, consequently, of the chemical potential ζ_0 can be determined from Eq. (10) with $S_m=2\pi m^*\zeta_0$. The experimentally determined values of m^* are given in Table I; the value $m^*/m_0=0.065$ is adopted as a good average of those. This value, together with the other parameters obtained from the present work for the group of light holes, is shown in Table II, along with corresponding results from other techniques.

B. Fluctuation in the Period of the Light-Hole Ellipsoid

Despite the very good agreement between the present mapping of the light-hole ellipsoid and the one of Brandt, as well as the good match between the effective mass found here and the one found by cyclotron resonance and anomalous skin effect determinations, some doubt still exists about some of the characteristics of this pocket:

(a) Most of the analyses of galvanomagnetic effects with a two-band model seem to indicate a smaller number of holes, $n_h\approx2.5\times10^{17}$ cm^{-3}, (see the two-band model in Sec. VE) than found in the light-hole mapping; (b) a possible departure from ellipsoidal shape is indicated in the first report of Brandt *et al*[15]; (c) lately, an indication has been given by Lerner[23] of the existence of isotropic periods 7.2×10^{-6} G^{-1} appearing mostly for large values of ψ. These periods are interpreted by Lerner as those of the heavy-carrier ellipsoid. Should they be interpreted as belonging to the light-hole pocket with the period 7.0×10^{-6} G^{-1} replacing the extrapolated 4.3×10^{-6} G^{-1} value, the result would be a number of carriers close to the value expected from the two-band model.

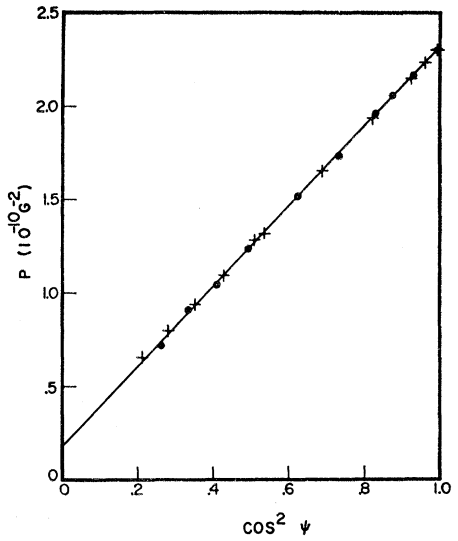

FIG. 5. P^2 versus $\cos^2\psi$ for the light-hole ellipsoid. Data were taken at 1.8°K. The straight line corresponds to an ellipsoid with ratio of major to minor axis 3.59.

A careful investigation of the period of the light holes was performed again with the field in the (2)–(3) plane, mostly for large values of ψ. With ψ in the range 0 to 30°, perfect monoperiodic oscillations were seen in most of the field range with an appearance at high field of a slight distortion of the oscillations interpretable either in terms of the appearance of a second harmonic or in terms of Lerner's isotropic period. For higher ψ values, 30° to 60°, a slight modulation appears in the periods as a function of the field; the period of the modulation seems to correspond to the longest period of the electron pockets. Since the modulation amplitude is small, the average period obtained by fitting a straight line to the $\psi=63°$ data in Fig. 4 still can be considered as a suitable determination for the mapping parameters.

For ψ greater than 60°, the galvanomagnetic oscillations decrease in amplitude; the range of field for which they are detectable rarely exceeds the range in which the modulation occurs. A field-dependent period is then obtained in the analysis. In the case of the largest ψ angle, instead of a smooth variation in period,

TABLE I. The cyclotron mass m^*/m_0 of the hole ellipsoid, with the magnetic field parallel to the trigonal axis, obtained from the temperature dependence of the oscillation amplitude in the Hall conductivity σ_{12} and magnetoconductivity σ_{11}, respectively, at different magnetic-field values.

Magnetic-field values (H) (kG)	From temperature dependence of $\tilde{\sigma}_{12}$	From temperature dependence of $\tilde{\sigma}_{11}$
10	0.0647	0.065
12	0.0636	0.0694
14	0.0658	0.0639

TABLE II. Direct data from various measurements on high-mobility holes ellipsoid. The characteristic parameters of the hole ellipsoid. Some of the earliest data on the ellipsoid are indicated.

	Present work	dHvA effect Brandt[a] *et al.*	Cyclotron resonance Galt[b] *et al.*	Anomalous skin effect Smith[c]	Hall effect Reynolds[d] *et al.*
S_{II} (10^{-42} g^2 cm^2 sec^{-2})	6.97	6.75	...	...	...
$S_{\perp}$ (10^{-42} g^2 cm^2 sec^{-2})	25.02	25.75	...	...	...
$S_{\perp}/S_{II}$ ($=R$)	3.59	3.81	...	...	...
n (10^{17} holes cm^{-3})	3.43	3.4	...	...	...
ζ_0 (10^{-14} erg)	1.9	2.5	...	...	2.0
m_3/m_0	0.065	0.05	0.068	...	0.062
m_1/m_0	0.84	0.7	0.92	...	...
m_1/m_3 (R^2)	12.9	14	13.5	12.8	...

[a] See Ref. 16.
[b] See Ref. 12.
[c] See Ref. 8.
[d] See Ref. 18.

the variation appears almost discontinuous as if the electron oscillation were approaching the extreme quantum limit. The determination of an average period is then questionable. The experimental values for the periods are plotted versus ψ in Fig. 6. For $\psi \lesssim 50°$, the data are in excellent agreement with the form of Eq. (15). For $\psi \gtrsim 50°$, a considerable scatter in the data is apparent. Many of the data points fall into the range by Lerner.[23] (Lerner has recently indicated that the period and size of this pocket would be very sensitive to impurity and thus they would vary greatly from one sample to the next.) The existence of the heavy-carrier pocket discussed by Lerner is neither confirmed nor rejected; the scatter of the data calls for caution. For a two-band model with one hole ellipsoid and three electron ellipsoids as shown in Fig. 7, some explanation is found for this behavior of the period. When the magnetic field is in the direction of the binary axis ($\psi = 90°$), two of the electron ellipsoids present very small cross sections to the field. For field strengths somewhat above 25 kG, the last Landau level is above the Fermi energy so that no states are available for electrons in the two ellipsoids. In a first approximation, if n_e is the initial number of electrons per ellipsoid, the third electron ellipsoid must increase its population to n_e' and the hole-ellipsoid population must decrease from $n_h = 3n_e$ to $n_h' = n_e'$. The new extremal cross-sectional area S_m' of the hole ellipsoid is then smaller than the original value S_m; the associated relative increase in period is given by

$$P'/P = (\zeta_e + \zeta_h)/(3^{2/3}\zeta_e + \zeta_h), \tag{16}$$

where the ζ's are the respective chemical potentials. This corresponds to an increase of the period by about 60%. The fields used here were lower than those necessary for the extreme quantum limit; but the emptying of the two electron ellipsoids progresses in a manner periodic with increasing field.

With the phase from Eq. (9) written in the form

$$\frac{\phi'}{2\pi} = \frac{cS_m'}{eh}\left(\frac{1}{H}\right) + \frac{\phi_0'}{2\pi},$$

where S_m' is the field-dependent cross section of the hole

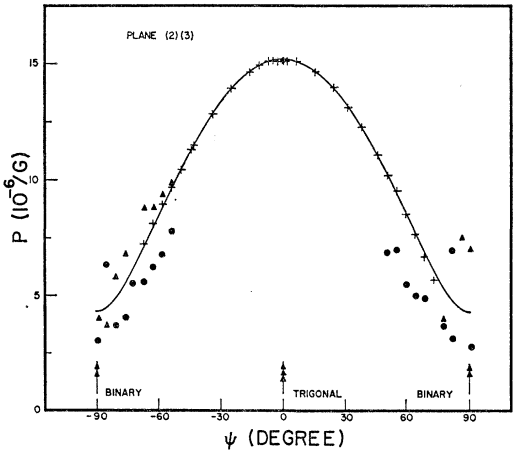

FIG. 6. The period P of the hole ellipsoid versus the orientation with emphasis for the large value of ψ on the indetermination of the period. (+) period average over the entire field range, (○) averaged period for lowest field, (●) averaged period for highest field. The solid line corresponds to the ellipsoid specified in Sec. VA.

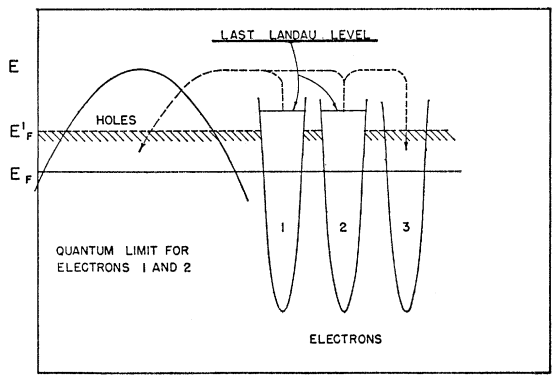

FIG. 7 Schematic representation of the holes and electrons in an E versus k diagram. When the electrons pockets (1) or (2) (or both) are emptied, the Fermi energy rises with an increase in number of electrons in pocket (3) and a decrease in the number of holes.

ellipsoid, comparison can be made with the phase ϕ expected from a fixed S_m value

$$\frac{\phi}{2\pi}=\frac{cS_m}{eh}\left(\frac{1}{H}\right)+\frac{\phi_0}{2\pi}.$$

In Fig. 4 for $\psi=63.6°$, the values of $\phi/2\pi$ and $\phi'/2\pi$ plotted versus $1/H$ are represented by the straight line for $\phi/2\pi$ and by the experimental points for $\phi'/2\pi$, respectively. The relative deviation is

$$\frac{\phi'-\phi}{\phi-\phi_0}\approx\frac{\Delta S_m}{S_m}\approx\frac{2}{3}\frac{\Delta n_h}{n_h},$$

with $\Delta n_h/n_h$ the relative variation of the number of holes in the hole pocket. The above is also in first approximation

$$\frac{\Delta\phi}{\phi-\phi_0}=\frac{4}{9}\left\{1+\frac{1}{3}\frac{\zeta_h}{\zeta_e}\right\}^{-1}\times\frac{\Delta n_e}{n_e}\approx 0.36\frac{\Delta n_e}{n_e}, \quad (17)$$

where $\Delta n_e/n_e$ is the relative variation of the number of electrons in one of the electron pockets as the extreme quantum limit is approached. According to this equation, the fluctuation in the curve $\psi=63.6°$ of Fig. 4 seems to indicate an order of magnitude for $-(\Delta n_e/n_e)$ of 3 and 15% for $H=8$ kG and $H=15$ kG, respectively, values which can reasonably be expected from an expression for Δn_e similar to Eq. (9). Equation (17) must be modified to account for larger fluctuations. Departure from the quasicontinuous distribution of states in the hole pocket, directions of field different than that of the binary direction, and possible existence of other bands may need to be considered. Nevertheless, since fluctuations in ϕ' are important, the value of the apparent period P' as determined from measurements in a short range of field is affected appreciably since $1/P'=(1/2\pi)\partial\phi'/\partial(1/H)$. The wide scatter of the points in Fig. 6 may be a consequence of this mechanism; in which case, caution should be used in interpreting periods measured at high fields, over a short range of fields, for directions ψ greater than 60°.

C. Thermal Conductivity

Knowledge of the thermal-conductivity tensor is necessary for the computation of the kinetic thermoelectric coefficients. It is ordinarily computed from the experimental thermal resistivity coefficients.[34] Bismuth shows a particularly simple thermal-resistivity behavior with a practically field-independent γ_{11} term and a negligible γ_{21} Righi-Leduc resistivity ($G_2=0, \gamma_{21}=0$). This can be summarized by $\hat{\gamma}=\gamma_{11}\mathbf{1}$ and the conductivity give simply $\hat{\lambda}=\lambda_{11}\mathbf{1}$ with $\lambda_{11}=\gamma_{11}^{-1}$.

Data for the thermal conductivity at zero-magnetic field, along with earlier work on bismuth by Shalyt[46] and White and Woods[47] are presented in Fig. 8. The low-temperature points may be made to fit the T^3 behavior of lattice conductivity as expected when the size effect is preponderant. The conductivity seems to reach a maximum around 3.6°K, but more recent measurements on the same crystal[48] indicate a maximum around 4°K with a value of λ at 4.2°K about 12% higher than reported here.

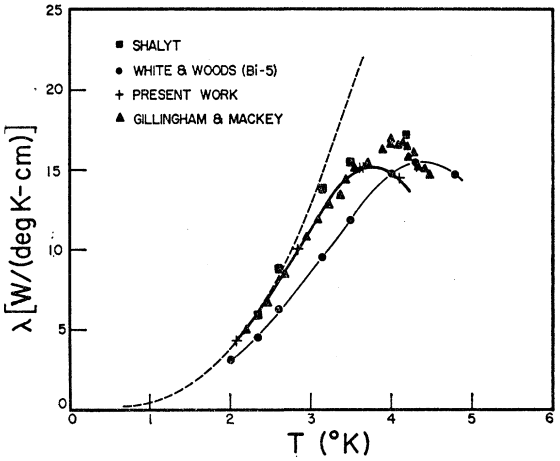

FIG. 8. The thermal conductivity in function of temperature for a zero-magnetic field. This conductivity is practically due to the lattice only. The dashed line is the expected low temperature T^3 variation adjusted to fit the data. Data of Schalyt (Ref. 46), White and Woods (Ref. 47), and Gillingham and Mackey (Ref. 48) are also given.

An indication of the contribution of the electrons to the heat flow is obtained from the Wiedemann-Franz law: At 4.0°K and zero field, the electronic part of the thermal conductivity is $\lambda_e=3.18\times10^{-2}$ W/deg-cm. By comparison with the data of Fig. 8 it is seen that the expected electronic contribution to the total thermal conductivity is only a fraction of 1%.

Measurements of λ with and without an external magnetic field served to substantiate the neglect of the electronic contributions. In the calculation of the tensor elements the heat conductivity is assumed to be due to the lattice only; thus, the thermal effects are described simply by

$$G_2=0;\quad w_1^*=\lambda_{11}G_1=\lambda_L G_1;\quad w_2^*=0,\quad \lambda_{21}=0. \quad (18)$$

If the mean free path Λ is established by scattering from the boundaries of the crystal, the expected value of the thermal conductivity, $\lambda_L=\frac{1}{3}C_L v\Lambda$, is 5.4 W/deg-cm at 2.07°K. Here the average sound velocity v and the lattice heat C_L are computed classically with a Debye characteristic temperature of 117°K.[24] This value compares favorably with the experimental value $\lambda_L=4.3$ W/deg-cm.

[46] S. Shalyt, J. Phys. USSR 8, 315 (1944).

[47] G. K. White and J. B. Woods, Phil. Mag. 3, 342 (1958).

[48] R. Gillingham, S.J. and H. J. Mackey (private communication); R. Gillingham, Ph.D. thesis, Louisiana State University, 1962 (unpublished); H. J. Mackey, Ph.D. thesis, Louisiana State University, 1963 (unpublished).

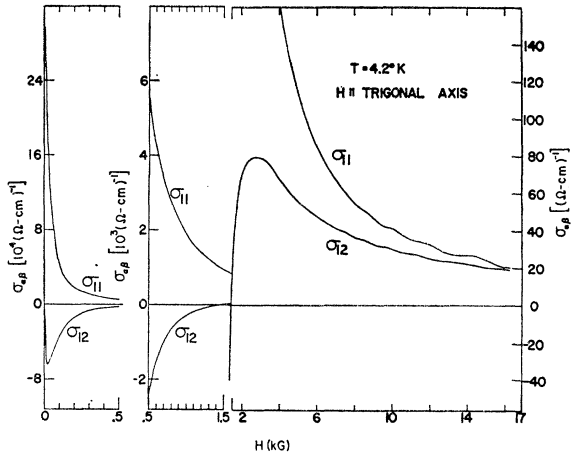

FIG. 9. The Hall conductivity and the transverse magnetoconductivity. The $\sigma_{\alpha\beta}$ over the complete range of H are shown by using three different scales. These curves were calculated from experimental data using Eq. (4).

It is of interest to note that dHvA type oscillations have been reported in the thermal resistivity of bismuth at 1.604°K,[26] but were not observed in the present study (minimum temperature 2.1°K) perhaps because of the impurity content of the sample.

D. Four-Band Model

The mobilities, populations, and densities of states of the various bands are obtained by the fitting to Eqs. (5) and (6) of the coefficients $\sigma_{\alpha\beta}$, Fig. 9, and $\epsilon_{\alpha\beta}''$, Fig. 10, determined from the experimental data. This process does not, in practice, completely solve the problem, but does give a useful indication of the various bands. A reasonably good fit can be obtained if only one of the quantities, say σ_{11}, is considered. If a simultaneous fit for all the tensor elements and a correlation

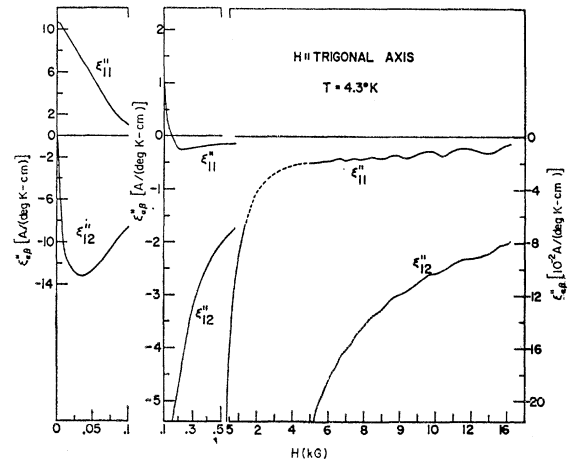

FIG. 10. The kinetic thermoelectric coefficient and the kinetic Ettingshausen-Nernst coefficient calculated from Eq. (4) in function of magnetic field. The $\epsilon_{\alpha\beta}''$ over the complete range of H are shown by using there different scales.

with the band parameters as determined from oscillation analysis, i.e., number of holes be equal to 3.4 $\times 10^{17}$ cm^{-3}, are required, serious discrepancies result. Table III gives the results of a deliberately short analysis of the curve fitting. Work is now underway in analyzing more complete field and temperature data to unravel many of the problems encountered in the present analysis.[48] The curve-fitting technique, in addition to requiring that the final results match the experimental $\sigma_{\alpha\beta}$ and $\epsilon_{\alpha\beta}''$, involves curve extrapolation at high- and low-field limits. The utility of these plots is evident from an expansion of Eqs. (5) and (6) in the high- and low-field limits.[48] Low-field extrapolations are made by the plotting of each of the quantities σ_{12}/H, ϵ_{12}''/H, ϵ_{11}'', and σ_{11}, versus H^2. For the high-field limit, the useful plots are $H\sigma_{12}$, $H\epsilon_{12}''$, $H^2\epsilon_{11}''$, and $H^2\sigma_{11}$ versus $1/H^2$. Further, the results should satisfy the fundamental requirements.[49]

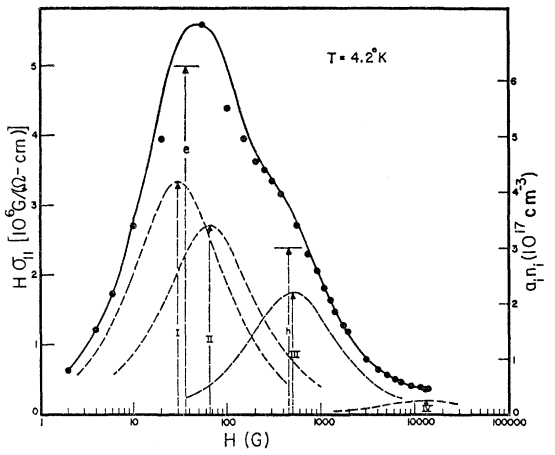

FIG. 11. $H\sigma_{11}$ versus $\ln H$ for $T=4.2$°K. The broken lines are representative of bands I, II, III, and IV, respectively, of the multiband model. The full line is the sum of the different bands constributions. The crosses represent experimental points. The right scale shows directly the apparent population of the bands $a_i n_i$. Bands (e) and (h) of the two-band model, which give a relative good fit of the experimental point, are also indicated.

$$\int_0^\infty \sigma_{11} dH = \tfrac{1}{2}\pi ec \sum a_j n_j;$$
$$\int_0^\infty \sigma_{12}/H dH = \tfrac{1}{2}\pi ec \sum (\pm) n_j/H_j. \tag{19}$$

The experimental evaluation of $\int_0^\infty \sigma_{11} dH$ yields a value $\sum a_j n_j = 10\times 10^{17}$ cm^{-3} at 4.2°K which, for example, eliminates the possibility of a multiplicity of 2 for the light-hole ellipsoid. It was found also that one of the most illustrative ways to plot the data was that of σ_{12}, $H\sigma_{11}$, ϵ_{12}'', $H\epsilon_{11}''$ versus $\ln H$, for which plots, the

[49] J. W. McClure, Phys. Rev. **112**, 715 (1958).

TABLE III. Parameters of the different bands in bismuth, when the different transport effects are decomposed into Lorentz terms using Eqs. (5) and (6). The italicised quantities have been forced into the analysis, for example the parameter of band II in the multiband model are those of the hole ellipsoid in Table II. Between parentheses are the values of the saturation field giving the best individual fit, for example $H_1=30$ $H_2=65$ best fit for the σ_{11} analysis in the determination of a_1n_1 and a_2n_2. Band (4) arises from the identification of the high-field behavior of some of the effects with a Lorentz term; it is common to the multiband and "two" band model.

	Multiband model				Two-band model	
	Electron (1)	Holes (2)	Holes (3)	Holes (4)	Electrons	Holes
H_i	30 to 35 G	60 to 65 G	~500 G	13 to 14 kG	28 to 35 G	300 to 450 G
n_i (10^{17} cm^{-3})	4.3 (32)	*3.4* (65)	1.1	~0.01	2.62 (29)	2.8 (300)
a_1n_i (10^{-17} cm^{-3})	4.3 (30)	*3.4* (65)	2.5	0.25	6.4 (35)	3 (450)
b_iZ_i (10^{31} cm^{-3} erg^{-1})	30 (30)	*2.7*	10	21	30 (30)	12
c_1Z_i (10^{31} cm^{-3} erg^{-1})	17 (35)	*2.7* (60)	7	11	15 (32)	7.5 (400)
ζ_i (10^{-14} erg)	*2.8*	*1.9*	0.42		*2.8*	*1.9*
Z_i (10^{31} cm^{-3} erg^{-1})	~2.4	2.7	7		1.4	2.2
a_i	1	*1*	~2.4		~2.5	1.1
b_i	~12	1	~1.5		~20	5.4
c_i	~7	*1*	*1*		~11	3.4

contribution of the various bands can be best visualized as in Figs. 11–13 for $H\sigma_{11}$, $H\epsilon_{11}'$, and σ_{12} at 4.2°.

(1) The high-mobility electron pocket ($H_1=32$ G) is identified with that discovered by Shoenberg from dHvA studies.[14] It should also be compared to the electrons of the two-band model interpretation of the galvanomagnetic effects, cyclotron resonance, and anomalous skin effect. Some of the experimental values of n_1 obtained by various means are shown in Ref. 50. There is a general agreement between the value of 4.3×10^{17} electrons cm^{-3} reported in Table III [Electrons (1)] and those listed in Ref. 50. There is still ambiguity as to the multiplicity of the electron ellipsoids since very different values for the number of electrons per ellipsoid have been given, even recently. A value $n_e=0.91\times10^{17}$ cm^{-3} per ellipsoid may favor a 6 ellipsoid set; a value $n_e=1.4\times10^{17}$ cm^{-3}, a 3 ellipsoid set.

One difficulty in the identification of band (1) with the electrons of Shoenberg's ellipsoids comes from the experimental result $a_1n_1\approx n_1$, which would indicate an isotropic band. The value of a_1 as obtained from various

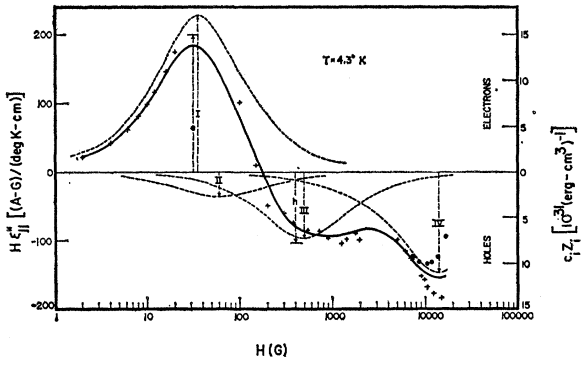

FIG. 12. $H\epsilon_{11}''$ versus $\ln H$ for $T=4.3$°K. The broken line curves are representative of bands I, II, III, and IV, respectively, of the multiband model, the full line is the algebraical sum of those bands' curves. The right scale measures directly the apparent density of state of each c_iZ_i. Bands (e) and (h) of the two-band model which give a relatively good fit of the experimental point are also indicated. Oscillations in the high-field range are indicated by some of their maxima (○) and minima (+).

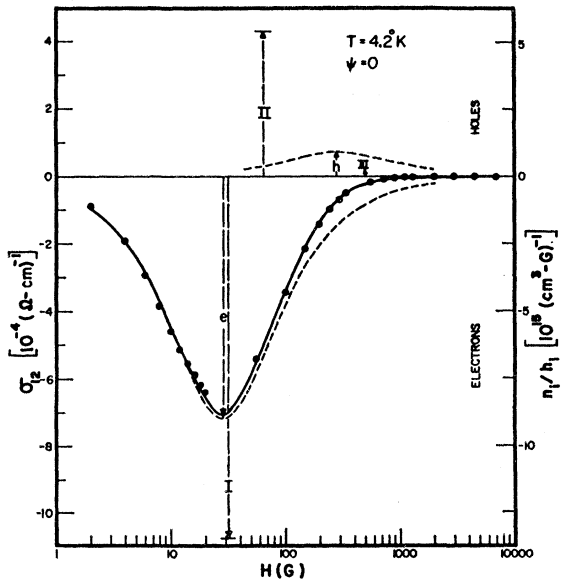

FIG. 13. σ_{12} versus $\ln H$ at $T=4.2$°K. The broken-line curves are representative of the electron band (e) and hole band (h) of the two-band model. The full line is the combined effect of the two. The points represent some of the experimental values. The right scale shows directly the size of the band as measured by n_i/H_i in G^{-1} cm^{-3}. Also bands I, II, and III of the multiband model are indicated.

[50] The number of electrons per ellipsoid measured directly may vary if correction for nonparabolicity and nonellipticity [Morrel H. Cohen, Phys. Rev. **121**, 387 (1961)] are made. Some of the values are $(0.91, 0.95, 1.01, 1.09, 1.25, 1.4)\times10^{17}$ cm^{-3} per ellipsoid from Refs. 11, 17, 23, 23, 14, and 4, respectively. From the two-band model interpretation of cyclotron resonance, or effect of alloying, the total number of electrons will be [4.6 (80°K), 4.9, 5.5, 5.8, 2.5, 3.9, 4.2]$\times10^{17}$ cm^{-3}, as given in Refs. 1, 2, 8, 17, 7, 4, and 12, respectively.

experimental data[51] ranges from 3.22 to 11 with an average value about 5. However, because of the high mobility and the restriction of Eq. (19) which excludes another densely populated band of electrons, band (1) must be designated as Shoenberg's ellipsoids and $a_1 \approx 1$ result must be considered as an anomaly, yet unexplained. Probably removal of the restriction that τ be isotropic and independent of energy would bring the theory more in line with experiment. Another surprising result in this band is the extremely large value of $b_1 Z_1$, which is 12 times the expected value $\frac{3}{2} n_1/\zeta_1$, $(b_1=1)$, where n_1 and[52] ζ_1 are taken from Table III. This anomalously large value for the density of states may account for the anomalously large specific heat (see Sec. VE), a fact which, if true, is unexpected and which at present is not understood. Work on an unexpected temperature dependence of the parameters of this band may help clear this point.[48] Only the $c_1 Z_1$ value approaches theoretical expectation[51] with $c_1=7.0$. The condition $c_1=a_1$ is far from being established experimentally since a_1 is apparently anomalous.

(2) Band (2) is logically identified as the single ellipsoid of light (high-mobility) holes, described in Sec. VA. The sign (+) and population of the band, as well as the comparison of its effective mass to that of the light-electron band[53] ($H_1/H_2 \approx m_1^*/m_2^*$, the same τ assumed for each) contribute to this identification. Thus the value $n_2=3.4\times10^{17}/\text{cm}^3$ has been adopted even though a more recent investigation[48] shows a slightly better fit with n_2 somewhat smaller. The adopted value of $H_2=65$ G is a compromise—a smaller value is called for in the ϵ_{11}'' curve fitting, but there is a degree of uncertainty here due to the nearness of band (3). In the ϵ_{11}'' and ϵ_{12}'' fitting, the effect of these light holes can hardly be seen, which indicates there is no anomaly in the density of states as with the light-electron band. In fact, the apparent density of states here is only 10% of that of the light electrons. Since the FS for this band is circular in the basal plane, we have set a_2, b_2, and c_2 equal to unity. Recent experiments[48] indicate that a value of $b_2 \approx 1.5$ may be more appropriate.

(3) The third band consists of rather low-mobility holes ($H_3 \simeq 500$ G). The population of this band n_3 has been determined only within limits: Contradictory evidence sets n_3 between 0.7×10^{17} and 2.5×10^{17} cm^{-3}. A careful weighing of the evidence gives $n_3 \approx 1.1\times10^{17}$ cm^{-3} and $a_3 n_3 \approx 2.5\times10^{17}$ cm^{-3} for the most suitable concentration. In any case, these values are smaller than the value of 2.88×10^{17} cm^{-3} obtained by Lerner.[23] It is worthy of note that the presence of band (2) and the parameters adopted for it influence the parameters of band (3) to such an extent that many investigators have considered only a single band of holes. A band of low-mobility carriers such as band (3) is needed to explain the high density of states in bismuth as seen from specific heat data. Nevertheless, as indicated in Table III, the contribution to the density of states by this band (as determined by both Ettingshausen-Nernst and thermoelectric data) is, although large, only about $\frac{1}{2}$ the apparent contribution of the light electrons. If this band is composed of a single isotropic pocket as suggested by Lerner,[23] one should set $a_3=b_3=c_3=1$. For $n_3 \approx 1.1\times10^{17}$ and $Z_3 \approx 7\times10^{31}$, the chemical potential is $\zeta_3=0.235\times10^{-14}$ ergs (Fermi temperature of 13°K) and the effective mass is $m_3^* \approx 0.57 m_0$. The existence of more than one pocket in the third band would force a larger value for m_3^* and a smaller value for the Fermi temperature T_3. An indication of the effective cyclotron mass for the carriers in this band is obtained if equal relaxation times for all carriers are assumed. With H_1, H_2, and H_3 given by 32, 65, and 500 G, respectively, and m_1^* and m_2^* given by $0.055 m_0$ and $0.065 m_0$, respectively, the effective cyclotron mass values of $m_1^* H_3/H_1=0.8 m_0$ and $m_2^* H_3/H_2=0.5 m_0$ fall quite close to the above value for the isotropic effective mass m_3^*.

(4) Band (4) does not have the same significance as the other three: The maximum contribution of this band to the transport processes appears at high field ($H_4 \approx 13$ kG) in the range where the oscillations are important. In this magnetic field range, the semiclassical theory is no longer applicable, except for the asymptotic behavior of σ_{12}. Indeed, very little evidence for this band can be shown from σ_{12}, the only clue being the existence of an extremely small concentration of holes ($n_4 \approx 0.015\times10^{17}$ cm^{-3}). In fact, more recent data on[48] σ_{12} gives a value for n_4 even smaller with limits of precision which make it impossible to distinguish between a hole or electron character for this carrier. Nevertheless, band (4) is analyzed in the usual manner, since considerations of σ_{11}, ϵ_{11}'', and ϵ_{12}'' indicate the existence of a band of the standard form. The low apparent number of carriers $a_4 n_4 \approx 0.25\times10^{17}/\text{cm}^3$ in σ_{11}, with practically no contribution in σ_{12}, along with the extremely large apparent density of states seems to indicate the band may be due to impurities or to a departure from the simple theory used here. The hole character is mainly indicated by the sign of the ϵ_{11}'' thermoelectric data

In summary, the band structure of bismuth can be explained by four distinct bands, three of them with the usual character due to groups of carriers. An

[51] The weighting factor a_1[37] (or c_1), the ratio between linear average and rms average of the mobility in the (1)–(2) plane for electrons, can be computed from data of different authors: 11.3, 4.5, 4.6, 5.35, 6.35, 3.22, 5.55, 4.75, etc. See Refs. 14, 12, 10, 11, 23, 1, 14, and 4, respectively.

[52] Shoenberg's value (Ref. 14) 2.8×10^{-14} ergs is used here as the value of the chemical potential ζ_e. This value is in agreement with Lerner's (Ref. 23). The nonparabolic model correction [see Cohen, Ref. 50)] leads to the somewhat different values $(3.5, 4.2)\times10^{-4}$ ergs per electron. See Refs. 17 and 23, respectively.

[53] The cyclotron mass for the electrons in the (1)–(2) plane has been directly measured by cyclotron resonance $(0.08, 0.051)\times m_0$ (see Refs. 12 and 13, respectively) or can be computed from different effects. $m_e^*=0.055 m_0$ has generally been the value adopted for best fit (Refs. 14, 10, 11, 17, 23). Then $m_1^*/m_2^*=0.85$ as compared to $H_1/H_2=0.5$.

illustration of the contributions of the various bands to the observed effects can be seen in Figs. 11–13. In Fig. 12 the quantity $H\epsilon_{11}''$ is plotted as a function of $\alpha=\ln H$. The contribution of each band is a uniform curve of the form $A_j\,\mathrm{sech}(\alpha-\alpha_j)$ where $A_j=(\pi^2k^2cT/6)\times(c_jZ_j)$. The sum of the four curves coincides very nearly with the experimentally observed values as shown in Fig. 12. Similarly, the quantity $H\sigma_{11}$ is displayed in Fig. 11 as the sum of the contributions from each of the four bands. It should be noted that in similar plots of the transverse effects σ_{12} and ϵ_{12}'', more importance is attached to the higher mobility bands. This is the case since σ_{12} and ϵ_{12}'' directly exhibit the quantities n_j/H_j and b_jZ_j/H_j, respectively, as seen in Fig. 13.

E. Density of States and Specific Heat

The electron specific heat is known to be a direct measure of the total density of states, $C=\frac{1}{3}\pi^2k^2TZ$. In the case of bismuth, a strangely large value of the specific heat ($Z=50\times10^{31}$ erg^{-1} cm^{-3}) has been found by Kalinkina and Strelkov.[24] More recent measurements by Phillips[25] indicate a smaller value, with $Z=15.5\times10^{31}$. The apparent density of states as determined from Table III is (in units of cm^{-3} erg^{-1}) $\sum b_jZ_j\approx64\times10^{31}$, $\sum c_jZ_j\approx38\times10^{31}$, in reasonably good agreement with Kalinkina and Strelkov. However, assuming the possibility of the fourth band being due to impurities, one would obtain $\sum_1^3 b_jZ_j\approx43\times10^{31}$, $\sum_1^3 c_jZ_j\approx27\times10^{31}$ for very pure bismuth. Furthermore, if the abnormally large value of $b_1Z_1\approx30\times10^{31}$ is rejected and the expected value of $Z_1=2.4\times10^{31}$ substituted, a result $Z=Z_1+Z_2+b_3Z_3=15.1\times10^{31}$, is obtained as a reasonable value for very pure bismuth; in excellent agreement with the results of Phillips.[25] No attempt is made here to take account of the nuclear quadrupole contribution to the specific heat.[23–25]

F. Two-Band Model

A relatively good fit of the experimental data is attained with only a two-carrier model. Evidently, the pseudoband which appeared in the preceding analysis as band (4) will appear here too; but as already pointed out, no carriers seem to correspond to it. Thus attention is given only to the contributions of the other bands. The fact that bands (1) and (2) of the preceding analysis are so close together make possible the consideration of the two as a single one in first approximation. The hole band (3) of the former analysis is slightly more populated and slightly more mobile. The results of the two-band model analysis are shown in Table III. The number of electrons is close to the value found from low-field galvanomagnetic effects.[50,7] The excess of holes over the electrons is most probably due to some acceptor impurities. The weighting factor[37] a_e for electrons is in better agreement with the expected value[51] than in the former case of the multiband model; but the ratio between the hole and electron mobility $H_e/H_h\approx0.1$ is much too small compared to the expected value[53] of 0.85. The holes play a role more in agreement with the heavy holes suggested from different studies[2,23,25] and are by comparison to the electrons, much too heavy to be identified with the light-hole ellipsoid (Sec. VA).

The identification of the light-hole ellipsoid (with its chemical potential of 1.9×10^{-14} ergs) leads to a density of state 3.4 to 5.4 times smaller than the apparent values obtained from the Nernst-Ettinghausen thermoelectric effects. As in the multiband case, an extremely large apparent density of state also appears in the Nernst-Ettinghausen effect for the electrons ($b_e\approx20$).

There is no doubt that the analysis of the thermoelectric effects by terms of the type of Eq. (6) should give only a rough determination of the density of states. Any dependence of the relaxation time on field, energy and momentum will influence these effects even more than in the case of the galvanomagnetic effects. A more comprehensive analysis of these effects is now underway.[48]

G. Oscillations in the Galvanomagnetic Effects

Examination of the Lifshitz-Kosevich theory, Eqs. (7), (8), and (11), for $\tilde{\sigma}_{12}$ shows that no oscillations should appear at high magnetic field values where all bands are asymptotic. This is evident since the classical mobility $(\pm)ecH(H^2+H_j^2)^{-1}$ reduces to $q_{mj}{}^{12}\langle q_j^{12}\rangle_{\mathrm{av}}$ $(\pm)ec/H$ for $H\gg H_j$. Experimentally, the oscillations are quite pronounced in the high field range, as shown in Figs. 9 and 14. The implication is that some band (or bands) in bismuth has not reached its asymptotic value in the range of fields used in the experiments. Suppose there is one low-mobility band ($j=u$) which enhances these high-field oscillations. If the relaxation time is assumed independent of the energy, Eq. (7) can be written from Eqs. (8), (11), and (5) as

$$|\tilde{\sigma}_{12}|_{\mathrm{L-K}}=ec\sum\sum\left\{\frac{H}{H^2+H_j^2}-\frac{H}{H^2+H_i^2}\right\}\frac{Z_i}{Z}(\pm)_j\tilde{n}_j, \quad (20)$$

where $Z=\sum Z_i$. In the trigonal direction only oscillations due to the light holes ($j=2$) are observed. Since for high fields, H_j of the light holes and electrons can be neglected so

$$|\tilde{\sigma}_{12}|_{\mathrm{L-K}}=\frac{ec}{H}\tilde{n}_2\frac{H_u^2}{H^2+H_u^2}, \quad (21a)$$

where Z_u/Z is taken as unity. With $\tilde{n}_2$ taken from Eq. (9) and the experimentally determined values of λ and R, Eq. (21a) is solved for H_u. In taking only the first

TABLE IV. Comparison of the amplitude of the oscillations in the conductivity coefficients $|\tilde{\sigma}_{11}|_{\text{exp}}$, $|\tilde{\sigma}_{12}|_{\text{exp}}$ with the Lifshitz and Kosevich theory. Equations (22), (24), (21b), (25) are used to determine some characteristic parameters of the unasymptotic band, for different values of the magnetic field.

H (kG)	$\lvert\tilde{\sigma}_{11}\rvert_{\text{exp}}$ $(\Omega\ \text{cm})^{-1}$	$\lvert\tilde{\sigma}_{12}\rvert_{\text{exp}}$ $(\Omega\ \text{cm})^{-1}$	H_u/a_u (kG)	a_uH_u (kG)	H_u (kG)	a_u	Z_4/Z ($H_4=13$ kG)	a_4
10	2.17	0.79	3.63	4.15	3.88	1.07	0.205	3.58
12	2.25	0.82	3.67	4.60	4.11	1.12	0.195	3.54
14	2.6	0.9	3.46	5.95	4.54	1.31	0.205	3.76

term in the summation of Eq. (9), one obtains

$$|\tilde{\sigma}_{12}|_{\text{L-K}}=0.110H^{1/2}\lambda(\sinh\lambda)^{-1}\frac{H_u^2}{H^2+H_u^2}\ \text{in}\ (\Omega\ \text{cm})^{-1}. \quad (22)$$

The values of H_u obtained when this term is identified with the experimental amplitude, for various values of H, are given in Table IV.

The coefficient σ_{11} can be examined in a similar manner. With all bands asymptotic except one, we obtain

$$|\tilde{\sigma}_{11}|_{\text{L-K}}=(\mp)\frac{ec}{H}\tilde{n}_2\frac{a_uH_uH}{H^2+H_u^2}, \quad (23)$$

$(-)$ if the unasymptotic band is holes, $(+)$ if electrons. In this approximation, the ratio of oscillation amplitudes is

$$|\tilde{\sigma}_{11}|_{\text{L-K}}/|\tilde{\sigma}_{12}|_{\text{L-K}}=a_uH/H_u. \quad (24)$$

However, as seen in Fig. 14, there is an apparent difference in phase between the oscillation in $\tilde{\sigma}_{12}$ and $\tilde{\sigma}_{11}$; at high field, the phase difference approaches $\pi/2$, where a relative phase of π would be expected if the unasymptotic band were a hole band. Values for H_ua_u, a_uH_u, H_u, a_u are summarized in Table IV as determined, respectively, from Eqs. (22), (23), and (24) for data taken at 2.1°K. Note from the table that the experimental value of H_u increases with H. This is expected from this analysis if there are actually two bands (H3 and H_4) which are not asymptotic. The lower saturation field $H_3\approx 500$ G is indicated in the curve-fitting techniques and is substantiated in the next section by a comparison of the oscillation amplitudes in σ_{12} and ϵ_{12}''.

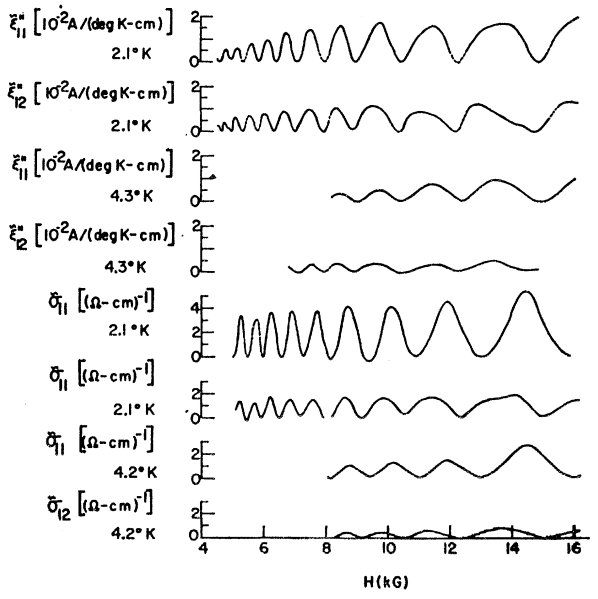

FIG. 14. The oscillatory components of the $\epsilon_{\alpha\beta}''$ and $\sigma_{\alpha\beta}$ at high fields at 2.1 and 4.2°K.

If, in the high-field range 10 kG$<H<$14 kG, the effects of the first three bands are neglected, Eq. (20) becomes

$$|\tilde{\sigma}_{12}|_{\text{L-K}}=\frac{ec\tilde{n}_2}{H}\frac{H_4^2}{H^2+H_4^2}\frac{Z_4}{Z}. \quad (21b)$$

Table IV gives the values of Z_4/Z calculated for $H_4=13$ kG as obtained from the curve fitting (Table III). The results compare favorably with the apparent value $b_4Z_4/bZ=0.32$ or $c_4Z_4/cZ=0.29$ computed from Table III. A smaller value of H_4 would bring Z_4/Z closer to these values.

With all bands asymptotic except $j=4$, the ratio of $\tilde{\sigma}_{11}$ to $\tilde{\sigma}_{12}$ is

$$|\tilde{\sigma}_{11}|_{\text{L-K}}/|\tilde{\sigma}_{12}|_{\text{L-K}}=a_4H/H_4. \quad (25)$$

The values of a_4 obtained from $H_4=13$ kG are given in Table IV. The difference between the values obtained here and those given in Table III are quite large but are of little significance since the parameters of the fourth band are quite indefinite. Although the nature of band (4) is not clear, the band enters in the Lifshitz-Kosevich theory in a straightforward manner.

H. Oscillations in the Thermoelectric Coefficients and in the Density of States

As has been indicated, $\epsilon_{\alpha\beta}''$ are calculated from the experimental $\epsilon_{\alpha\beta}'$ as shown in Fig. 3 by means of Eq. (4). With H parallel to the trigonal axis and the simplification due to Eq. (18), the tensor elements become

$$\begin{aligned}\epsilon_{11}''&=\epsilon_{22}''=\lambda_L[\sigma_{11}\epsilon_{11}'-\sigma_{12}\epsilon_{12}'],\\ \epsilon_{12}''&=-\epsilon_{21}''=\lambda_L[\sigma_{11}\epsilon_{12}'+\sigma_{12}\epsilon_{11}'].\end{aligned} \quad (26)$$

Calculated values of $\epsilon_{\alpha\beta}''$ display strong oscillations, as seen in Figs. 10 and 14.

For the high field oscillations in ϵ_{12}'', Eq. (6) is used

in the asymptotic form

$$\epsilon_{12}''=-\frac{\pi^2k^2cT}{3H}\sum Z_j. \tag{27}$$

If Eq (27) is valid in the quantum case, oscillations arise from the variations of the carrier's density of states. The oscillatory part of ϵ_{12}'' for band j=2 only is obtained by inserting Eq. (12) into Eq. (27) as

$$\tilde{\epsilon}_{12}''=\frac{\pi^2k^2cT}{3H}\tilde{Z}_2, \tag{28}$$

where $\tilde{Z}_j=(\partial\tilde{n}_j/\partial\zeta_j)$. The most important term in Eq. (28) comes from the differentiation of the phase in $\tilde{n}_2$, see Eq. (9).

If only the $\kappa=1$ term in Eq. (9) is retained, the oscillation amplitude is

$$|\tilde{\epsilon}_{12}''|_{\text{d.s.}}=0.095TH^{-1/2}\lambda/\sinh\lambda \text{ in A/deg-cm.} \tag{29}$$

The data of Table V show that at 2.1°K the expected

TABLE V. Comparison between the amplitude of the oscillation in the experimental Nernst-Ettinghausen kinetic coefficient $|\tilde{\epsilon}_{12}''|_{\text{exp}}$ and the amplitude of the oscillation $|\tilde{\epsilon}_{12}''|_{\text{d.s.}}$ due to the incidence in Eq. (28) of oscillation in the density of states, at different temperatures and for different magnetic field values. [Units of 10^{-6} A (°K cm)$^{-1}$.]

H	$T=2.1$°K		$T=4.2$°K	
(kG)	$\lvert\tilde{\epsilon}_{12}''\rvert_{\text{d.s.}}$	$\lvert\tilde{\epsilon}_{12}''\rvert_{\text{exp}}$	$\lvert\tilde{\epsilon}_{12}''\rvert_{\text{d.s.}}$	$\lvert\tilde{\epsilon}_{12}''\rvert_{\text{exp}}$
6	600	3500	90	
8	900	5000	300	1650
10	1100	5250	600	1750
12	1180	5250	880	1750
14	1200	6000	1120	2500
16	1220	6750	1320	

magnetic field dependence is followed quite well by the experimental data. However, the experimental values differ by a factor of 5 from those expected from this simplified theory. At 4.3°K, the values of $\tilde{\epsilon}_{12}''$ predicted by the theory differ from experimental values by a lesser margin; however, the agreement in the field dependence is not as good as that at 2.1°K. The predicted temperature variation is not observed.

The oscillations in ϵ_{12}'' are related to those in σ_{12} by Eqs. (9), (21a) and (28) as

$$|\tilde{\epsilon}_{12}''|_{d.s.}=i\frac{4\pi^2k^2cm^*}{3e^2h}\frac{T}{H}\left(1+\frac{H^2}{H_u^2}\right)|\tilde{\sigma}_{12}|_{\text{L-K}}$$

$$=i\frac{\pi k\lambda}{3e}\left(1+\frac{H^2}{H_u^2}\right)|\tilde{\sigma}_{12}|_{\text{L-K}}, \tag{30}$$

where $\kappa>1$ terms of Eq. (9) have been neglected and all bands are assumed asymptotic except one characterized with H_u and $Z_u=Z$.

As shown in Fig. 14, the oscillation of ϵ_{12}'' are shifted in phase by $\pi/2$ relative to those of σ_{12}, in excellent agreement with Eq. (30).

The experimental values for $\tilde{\epsilon}_{12}''$ and $\tilde{\sigma}_{12}$ substituted into Eq. (30) yield values for the low mobility saturation field $H_u=1.6$ kG at $H=10$ kG and $H_u=2$ kG at $H=14$ kG, both at 2.1°K. These values seem to indicate that the unsaturated third band plays a larger role than shown in Table IV.

Equation (12) is used to determine the effect of oscillations in the density of states on the thermoelectric coefficient for band $j=2$ only

$$|\tilde{\epsilon}_{11}''|_{\text{d.s.}}=|\tilde{\epsilon}_{11}''|_2\times\tilde{Z}_2/\bar{Z}_2. \tag{31}$$

This expression does not yield an amplitude as large as that expected from the contribution of scattering in the Zil'berman theory, see Eq. (11).

1. Oscillations in σ_{11} and ϵ_{11}'' and the Zil'berman Theory

In the Zil'berman theory, the oscillations due to a particular carrier depend on the characteristic parameters of that carrier alone; here, the light-hole band ($j=2$) parameters. Oscillation amplitudes for $|\tilde{\sigma}_{11})_{\text{Zil}}$ and $|\tilde{\epsilon}_{11}''|_{\text{Zil}}$ shown in Table VI are computed from Eqs. (13) and (14) at $T=2.1$°K for the following cases:

Case (a) The multiband model with the light-hole band as mapped in Sec. VA ($a_2=c_2=1$, $\bar{n}_2=3.4\times10^{17}$ cm^{-3}, $\bar{Z}_2=2.7\times10^{31}$ cm^{-3} erg^{-1}, $H_2=60$ G).

Case (b) The two-band model with the experimental parameters found in Sec. VF ($a_2\bar{n}_2=3\times10^{17}$ cm^{-3}, $c_2\bar{Z}_2=7.5\times10^{31}$ cm^{-3} erg^{-1}, $H_2=400$ G).

Case (c) The two-band model with isotropy imposed on band $j=2$ ($a_2=c_2=1$, $n_2=2.8\times10^{17}$ cm^{-3}, $Z_2=2.2\times10^{31}$ cm^{-1} erg^{-1}, $H_2=400$ G). In every case, λ_2 is computed with $m_2^*=0.065m_0$.

In Table VI, as shown for cases (a) and (b), the Zil'berman theory predicts the right order of magnitude for the $\tilde{\sigma}_{11}$ amplitude; the experimental values lie between those of case (b) and those of case (a). The experimental and predicted field dependences differ appreciably. It should be remembered that in the Lifshitz-Kosevich expression $|\tilde{\sigma}_{11}|_{\text{L-K}}$, matching can be obtained by adapting the parameter a_u or a_4 to the quite reasonable value 1.2 or 3.5, respectively. Probably both terms $\tilde{\sigma}_{11}|_{\text{L-K}}$ and $\tilde{\sigma}_{11}|_{\text{Zil}}$ contribute to the experimental oscillation.

Table VI also shows the expected values of $\tilde{\epsilon}_{11}''$ from the Zil'berman theory in the three cases. Agreement in the order of magnitude is achieved mostly in case (b) where the large apparent density of states for the holes is used; and thus favors the idea outlined in Sec. VF. In Table VI are also shown for comparison the amplitudes of oscillations expected in ϵ_{11}'' due to oscillations in the density of states. The amplitudes $\epsilon_{11}''/_{\text{d.s.}}$ for the optimum case (b) are shown to be negligible compared either to the experimental values or to the values calculated from the Zil'berman theory.

TABLE VI. Comparison of the amplitude of the oscillation in the experimental magnetoconductivity $|\tilde{\sigma}_{11}|_{exp}$ and kinetic-thermoelectric coefficient $|\tilde{\epsilon}_{11}''|_{exp}$ with the oscillation expected from Zil'berman's theory $|\tilde{\sigma}_{11}|_{zil}$, $|\tilde{\epsilon}_{11}''|_{zil}$, for the different cases. (a) $a_2=c_2=1$, $n_2=3.4\times10^{+17}$ cm^{-3}, $Z_2=2.7\times10^{31}$ cm^{-3} erg^{-1}, $H_2=60$ G; (b) $a_2n_2=3\times10^{17}$ cm^{-3}, $c_2Z_2=7.5\times10^{31}$ cm^{-3} erg^{-1}, $H_2=400$ G; (c) $a_2=c_2=1$, $n_2=2.8\times10^{17}$ cm^{-3}, $Z_2=2.2\times10^{31}$ cm^{-3} erg^{-1}, $H_2=400$ G. The σ are given in $(\Omega\ \text{cm})^{-1}$, the ϵ'' in 10^{-6} A $(°\text{K cm})^{-1}$. Also given, the $|\tilde{\epsilon}_{11}''|_{d.s.}$ shows the incidence in Eq. (31) of the oscillation in the density of states.

H (kG)	$\lvert\sigma_{11}\rvert_{exp}$ $(\Omega\ \text{cm})^{-1}$	$\lvert\sigma_{11}\rvert_{zil}$ a	b	$\lvert\tilde{\epsilon}_{11}''\rvert_{exp}$ $[10^{-6}$ A $(°\text{K cm})^{-1}]$	a	$\lvert\tilde{\epsilon}_{11}''\rvert_{zil}$ b	c	$\lvert\tilde{\epsilon}_{11}''\rvert_{d.s.}$ b
6	1.7	0.55	3.7	4320	216	4000	1180	55
8	2	0.62	4.2	7300	214	4000	1170	62
10	2.18	0.61	4.1	8370	180	3300	1000	60
12	2.25	0.56	3.7	7830	144	2450	720	53
14	2.6	0.5	3.2	8100	111	2030	600	48

With the different oscillatory effects written in the form

$$A\cos(2\pi/PH+\phi_0),$$

with A a positive amplitude; some comparisons can be made between the phase of each effect and the theoretical prediction. The value of ϕ_0 determined from experiment and theory are displayed in Table VII. The value of the period P used for the experimental determination of ϕ_0 was taken as 15.1×10^{-6} G^{-1}. There is some uncertainty in the phase determinations for $\tilde{\sigma}_{12}$ and $\tilde{\epsilon}_{12}''$ because these effects show some deformation in the high-field region. Thus for σ_{12}, two values of ϕ_0 are given, one for low and one for high field, -1.37π and -1.67π, respectively, with a somewhat good high-field fit of the value -1.75π expected from $|\tilde{\sigma}_{12}|_{L-K}$. The phase for $|\tilde{\sigma}_{11}|_{L-K}$ is for the case of an unsaturated hole band. The experimental $|\tilde{\sigma}_{11}|_{exp}$ matches well the Zil'berman value but some contribution of $|\tilde{\sigma}_{11}|_{L-K}$ is still possible. For $|\tilde{\epsilon}_{12}''|_{exp}$, two values of ϕ_0 are given, for low and high field: -1.82π and -2.0π, respectively, which are in fair agreement with the expected value -2.25π for $|\tilde{\epsilon}_{12}''|_{d.s.}$. A good agreement for the phase exists between $|\tilde{\epsilon}_{11}''|_{exp}$ and $|\tilde{\epsilon}_{11}''|_{zil}$; it was expected from Table VI that $|\tilde{\epsilon}_{11}''|_{d.s.}$ would not be influential.

In the above computations of the phase from theoretical expressions, the value of γ in Eq. (9) was taken equal to its free-electron value of $\frac{1}{2}$. An almost perfect fit would be obtained between theoretical and experimental effect with $\gamma=0.42$.

CONCLUSION

The properties of the crystal of bismuth used in this work, because of the relatively poor resistance ratio $R_{300°K}/R_{4.2°K}=40$, have the following simple features: Its thermal conductivity is practically all lattice conductivity; no size-effect correction has to be made for the galvanomagnetic effects; the residual resistance is attained at liquid-helium temperatures so that lattice-defect scattering can be assumed; the saturation fields of the different bands are in the magnetic field range most favorable for observation. However, the impurities in the crystal may be responsible for the appearance of a pseudoband, band (4), and the slight excess of holes over electrons.

The mapping of the light-hole Fermi surface agrees with that of Brandt and his co-workers as modified by the results of Galt *et al.* and those of Smith.

The band analysis of the different transport effects using a Lorentz term for each band can be made in either the case of two or three bands, plus the addition of a "pseudoband" in each case, to account for the high-field behavior. In both cases, a somewhat unusually high value of the apparent density of states is obtained for the light electrons. In the three-band model—one light-electron band (1), one light-hole band (2) and one heavy-hole band (3)—general agreement is obtained with the various data existent on bismuth, except for a very large uncertainty in the parameter of band (3) and the strange tendency for the light electrons to show an isotropic behavior. In the two-band model, difficulty exists for the identification of the hole band with the holes of the mapped ellipsoid. An unusual temperature dependence of the thermoelectric effects is found but not explained.

The oscillations in the different effects can be made to match or, at least, be of the order of magnitude of those expected from different theories. Thus the result of the Lifshitz-Kosevich theory for the oscillations in the Hall conductivity matches the experimental values when the empirically determined characteristics of band (4)

TABLE VII. Comparison between the phase of the oscillation in the experimental kinetic coefficient $|\tilde{\sigma}_{12}|_{exp}$ $|\tilde{\sigma}_{11}|_{exp}$ $|\tilde{\epsilon}_{12}''|_{exp}$ $|\tilde{\epsilon}_{11}''|_{exp}$ and the phase expected from the different theories (with the $\gamma=\frac{1}{2}$ free-electron assumption).

	$\lvert\tilde{\sigma}_{12}\rvert_{L-K}$	$\lvert\tilde{\sigma}_{11}\rvert_{L-K}$	$\lvert\tilde{\sigma}_{11}\rvert_{zil}$	$\lvert\tilde{\epsilon}_{12}''\rvert_{d.s.}$	$\lvert\tilde{\epsilon}_{11}''\rvert_{d.s.}$	$\lvert\tilde{\epsilon}_{11}''\rvert_{zil}$
Theoretical	-1.75π	-0.75π	-1.25π	-0.25π or -2.25π	-0.25π or -2.25π	-1.75π
Experimental average	-1.37π to -1.67π	-1.15π		-1.82π to -2.0π	-1.60π	

are used. The Zil'berman result for oscillation in the conductivity $\tilde{\sigma}_{11}$ matches the experimental values for conditions somewhat intermediate between the two and three band models, but the Zil'berman result for oscillation in the thermoelectric coefficient $\tilde{\epsilon}_{11}''$ favors the two-band model. The right order of magnitude for oscillation in the Nernst-Ettinghausen effect ϵ_{12}'' is obtained from the oscillations in the density of states.

ACKNOWLEDGMENTS

We are indebted to Dr. N. H. Zebouni and Dr. J. D. Childress for their help and useful discussions, to the members of the low-temperature group for their assistance, and most particularly to Dr. R. Gillingham, S.J., and H. J. Mackey who have kept us informed of their results.

PHYSICAL REVIEW VOLUME 132, NUMBER 1 1 OCTOBER 1963

Equation of State of Alkali Halides (NaCl)*

M. ARENSTEIN†
Autonetics, A Division of North American Aviation, Inc., Anaheim, California
AND
R. D. HATCHER AND J. NEUBERGER
Queens College, Flushing, New York

(Received 28 March 1963; revised manuscript received 17 June 1963)

The equation of state of NaCl is given using the Kellermann model of NaCl as well as a modified model making use of a repulsive potential energy of the Born-Mayer form Ae^{-Br}. The Grüneisen parameter $\gamma_i=-d\ln\nu_i/d\ln V$, where ν_i is the normal mode frequency and V is the volume, is derived by the development of a perturbation method in the volume. This is then used where needed to calculate all thermodynamic quantities of interest using an IBM 7090. A spectrum of 11 454 frequencies and γ_i's are used in finding these quantities rather than the approximations made previously of utilizing the elastic constants and the moment expansion $\gamma(S)=\Sigma_i\gamma_i\nu_i^S/\Sigma_i\nu_i^S=-(1/S)d\ln\langle\nu_i^S\rangle/d\ln V$, where $\langle\nu_i^S\rangle$ is the Sth moment of the frequency distribution. To check previous work by Barron and Blackman $\gamma(0)$, $\gamma(2)$, $\gamma(1)$, and $\gamma(-3)$ were calculated where $\gamma(0)=\gamma_\infty$, the high-temperature γ, and $\gamma(-3)=\gamma_0$, the low temperature γ. Fair agreement is found for $\gamma(-3)$, whereas the deviation in $\gamma(2)$ is high.

I. INTRODUCTION

THE equation of state of a real crystal such as NaCl has been considered by several investigators. Barron[1,2] and Blackman[3] using a Kellermann model[4] of NaCl and assuming equal masses for simplicity have recently obtained values for the low-temperature ($T\to 0$) Grüneisen[5] parameter γ_0. Barron was able to find a high-temperature ($T\gtrsim\Theta$, where Θ is the Debye temperature) Grüneisen parameter γ_∞ by defining a weighted γ in terms of the moments of the frequency spectrum with $\langle\nu_j^S\rangle$ the Sth moment

$$\gamma(S)=\sum_i\gamma_i\nu_i^S/\sum_i\nu_i^S=-\left(\frac{1}{S}\right)d\ln\langle\nu_j^S\rangle/d\ln V, \quad (1)$$

where

$$\gamma_i=-d\ln\nu_i/d\ln V \quad (2)$$

and ν_i is a normal vibration frequency, V is the volume, and the sum over i here and in all such expressions is to be taken over all normal modes of vibration. He found expressions for $\gamma(2)$ which he maintained should be approximately equal to $\gamma(0)\equiv\gamma_\infty$ and by making use of the elastic constants found a $\gamma_0=\gamma(-3)$. It was found that deviations from Grüneisen's relation should occur at 0.3Θ. Barron then compared his work to Born's[6] and Slater's.[7] Slater's formula, which is derived from a consideration of the elastic constants, is

$$\gamma_s=\tfrac{1}{2}d\ln(\chi V^{-1/3})/d\ln V, \quad (3)$$

where χ is the compressibility and V is the volume. This formula was derived under two assumptions, one being that Poisson's ratio is constant and the other that there is a characteristic temperature given by Debye's expression for an isotropic continuum,

$$\Theta=\frac{h}{k}\left(\frac{9N}{4\pi V}\right)^{1/3}\left(\frac{1}{C_l^3}+\frac{2}{C_t^3}\right)^{-1/3}, \quad (4)$$

* Work performed at New York University and partially supported by the U. S. Air Force.
† Much of the material included in this paper was used in a Ph.D. dissertation at New York University (1963).
[1] T. H. K. Barron, Phil. Mag. **46**, 720 (1955).
[2] T. H. K. Barron, Ann. Phys. (N. Y.) **1**, 77 (1957).
[3] M. Blackman, Proc. Phys. Soc. (London) **B70**, 827 (1957).
[4] E. W. Kellermann, Trans. Roy. Soc. (London) **238**, 513 (1940).
[5] E. Grüneisen, in *Handbuch der Physik*, edited by A. Geiger and Karl Scheel (Julius Springer-Verlag, Berlin, 1926), Vol. 10, p. 22.
[6] M. Born, *Atomtheorie des Festen Zustandes* (B.G. Teubner, Leipzig, 1923).
[7] J. C. Slater, *Introduction to Chemical Physics* (McGraw-Hill Book Company, Inc., New York, 1939), Chap. XIV.